



HAL
open science

AgRP Neurons Require Carnitine Acetyltransferase to Regulate Metabolic Flexibility and Peripheral Nutrient Partitioning

A Reichenbach, R Stark, M Mequinion, Rrg Denis, Jf Goularte, Re Clarke, Sh Lockie, Mb Lemus, Gm Kowalski, Cr Bruce, et al.

► **To cite this version:**

A Reichenbach, R Stark, M Mequinion, Rrg Denis, Jf Goularte, et al.. AgRP Neurons Require Carnitine Acetyltransferase to Regulate Metabolic Flexibility and Peripheral Nutrient Partitioning. Cell Reports, 2018, 22 (7), pp.1745-1759. 10.1016/j.celrep.2018.01.067 . hal-03105456

HAL Id: hal-03105456

<https://cnrs.hal.science/hal-03105456>

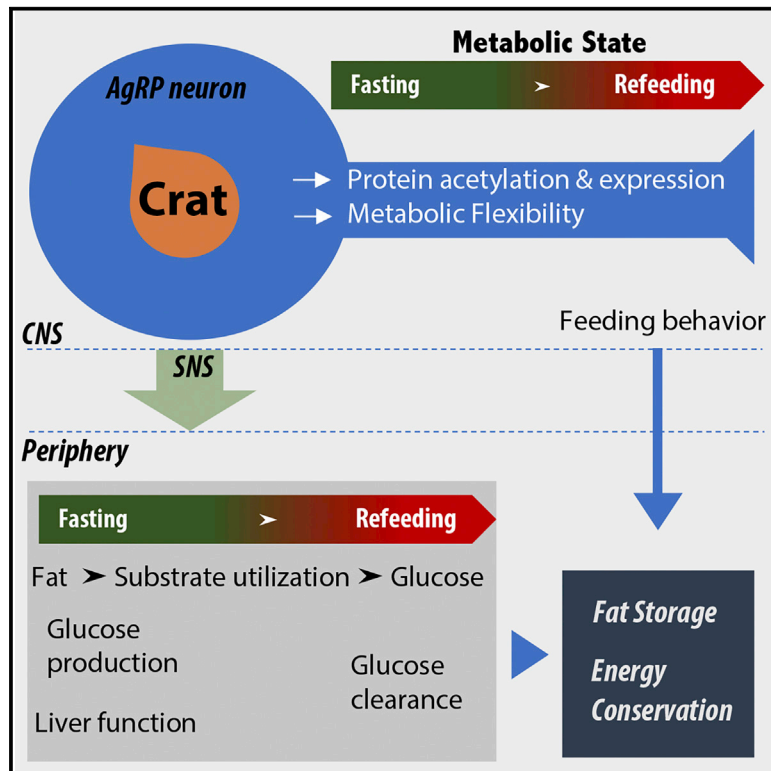
Submitted on 15 Nov 2022

HAL is a multi-disciplinary open access archive for the deposit and dissemination of scientific research documents, whether they are published or not. The documents may come from teaching and research institutions in France or abroad, or from public or private research centers.

L'archive ouverte pluridisciplinaire **HAL**, est destinée au dépôt et à la diffusion de documents scientifiques de niveau recherche, publiés ou non, émanant des établissements d'enseignement et de recherche français ou étrangers, des laboratoires publics ou privés.

AgRP Neurons Require Carnitine Acetyltransferase to Regulate Metabolic Flexibility and Peripheral Nutrient Partitioning

Graphical Abstract



Authors

Alex Reichenbach, Romana Stark, Mathieu Mequinion, ..., Matthew J. Watt, Serge Luquet, Zane B. Andrews

Correspondence

zane.andrews@monash.edu

In Brief

Reichenbach et al. demonstrate that AgRP neurons require carnitine acetyltransferase to regulate peripheral substrate switching from fatty acid to glucose utilization during fasting and the transition to refeeding. This mechanism preserves fatty acids when glucose from food becomes available and maximizes energy conservation for future periods of energy deficit.

Highlights

- Crat in AgRP neurons helps nutrient replenishment as food is available after fasting
- Crat in AgRP neurons helps maintain appropriate hepatic glucose production during fasting
- Crat in AgRP neurons facilitates peripheral substrate switching upon acute refeeding
- Crat regulates protein expression and acetylation in AgRP cells in fasting and refeeding



AgRP Neurons Require Carnitine Acetyltransferase to Regulate Metabolic Flexibility and Peripheral Nutrient Partitioning

Alex Reichenbach,^{1,2} Romana Stark,^{1,2} Mathieu Mequinion,^{1,2} Raphael R.G. Denis,³ Jeferson F. Goularte,¹ Rachel E. Clarke,^{1,2} Sarah H. Lockie,^{1,2} Moyra B. Lemus,^{1,2} Greg M. Kowalski,⁴ Clinton R. Bruce,⁴ Cheng Huang,^{1,5} Ralf B. Schittenhelm,^{1,5} Randall L. Mynatt,^{6,7} Brian J. Oldfield,^{1,2} Matthew J. Watt,^{1,2} Serge Luquet,³ and Zane B. Andrews^{1,2,8,*}

¹Monash Biomedicine Discovery Institute, Monash University, Clayton 3800, VIC, Australia

²Department of Physiology, Monash University, Clayton 3800, VIC, Australia

³Université of Paris Diderot, Sorbonne Paris Cité, Unité de Biologie Fonctionnelle et Adaptative, CNRS UMR 8251, 75205 Paris, France

⁴Institute for Physical Activity and Nutrition, School of Exercise and Nutrition Sciences, Deakin University, Burwood 3125, VIC, Australia

⁵Monash Biomedical Proteomics Facility and Department of Biochemistry, Monash Biomedicine Discovery Institute, Monash University, Clayton 3800, VIC, Australia

⁶Gene Nutrient Interactions Laboratory, Pennington Biomedical Research Center, Louisiana State University System, Baton Rouge, LA, USA

⁷Transgenic Core Facility, Pennington Biomedical Research Center, Louisiana State University System, Baton Rouge, LA, USA

⁸Lead Contact

*Correspondence: zane.andrews@monash.edu

<https://doi.org/10.1016/j.celrep.2018.01.067>

SUMMARY

AgRP neurons control peripheral substrate utilization and nutrient partitioning during conditions of energy deficit and nutrient replenishment, although the molecular mechanism is unknown. We examined whether carnitine acetyltransferase (Crat) in AgRP neurons affects peripheral nutrient partitioning. Crat deletion in AgRP neurons reduced food intake and feeding behavior and increased glycerol supply to the liver during fasting, as a gluconeogenic substrate, which was mediated by changes to sympathetic output and peripheral fatty acid metabolism in the liver. Crat deletion in AgRP neurons increased peripheral fatty acid substrate utilization and attenuated the switch to glucose utilization after refeeding, indicating altered nutrient partitioning. Proteomic analysis in AgRP neurons shows that Crat regulates protein acetylation and metabolic processing. Collectively, our studies highlight that AgRP neurons require Crat to provide the metabolic flexibility to optimize nutrient partitioning and regulate peripheral substrate utilization, particularly during fasting and refeeding.

INTRODUCTION

The maintenance of energy and glucose homeostasis requires the ability of the brain to detect and respond to acute changes in energy state. Under conditions of energy deficit, sensing low peripheral energy availability and hypoglycemia primes the brain to initiate food intake and increase hepatic glucose production (Kleinridders et al., 2009). Agouti-related peptide (AgRP) neurons

in the arcuate nucleus of the hypothalamus are a population of starvation-sensitive neurons that primarily function to increase appetite and promote energy conservation (Aponte et al., 2011; Gropp et al., 2005; Krashes et al., 2011; Luquet et al., 2005; Ruan et al., 2014). For example, adult ablation of AgRP neurons in mice causes a rapid cessation of food intake and profound body weight loss to the point of starvation (Luquet et al., 2005).

AgRP neurons primarily respond to signals of energy deficit and increase firing rates, mRNA expression, and peptide secretion (Andrews et al., 2008; Baskin et al., 1999; Briggs et al., 2011; Schwartz et al., 1998) to maintain energy homeostasis. Although AgRP neurons can respond to metabolic information in the form of hormonal feedback from ghrelin, leptin, and insulin (Andrews, 2011; Andrews et al., 2008; Enriori et al., 2007; Könnner et al., 2007; van de Wall et al., 2008; Wang et al., 2013), the mechanisms underlying nutrient sensing are less clear. This is not only important during fasting but also during the transition from fasting to refeeding when there is a dynamic change in metabolic feedback information to the brain. An appropriate level of metabolic flexibility ensures that, as glucose becomes available for oxidation, such as during refeeding, high fasting fatty acid utilization and oxidation are immediately suppressed to conserve energy reserves. Indeed, the ablation of AgRP neurons increases fatty acid utilization, affects nutrient partitioning, and attenuates body weight gain in mice fed a high-fat diet (Joly-Amado et al., 2012). Thus, the ability of AgRP neurons to rapidly adjust substrate utilization promotes maximal energy conservation and is a core component of nutrient partitioning. However, the molecular mechanism responsible for this action in AgRP neurons remains unknown.

Carnitine acetyltransferase (Crat) is an important enzyme regulating metabolic flexibility in muscle and increases exercise capacity (Muoio et al., 2012; Seiler et al., 2015). Crat is a fundamental enzyme in carnitine metabolism and is one of a number of



enzymes, including carnitine palmitoyltransferase 1 (CPT1) and carnitine octanoyltransferase, involved in regulating intracellular pools of acyl-coenzyme A (CoA) esters (Ramsay and Zammit, 2004; Stark et al., 2015a). In mice with muscle-specific deletion of *Crat*, excessive buildup of acetyl-CoA allosterically inhibits glucose oxidation by suppressing pyruvate dehydrogenase activity and impairs the substrate switch from fatty acid to glucose oxidation during the fast/refeeding transition (Muoio et al., 2012). Consequently, we hypothesized that *Crat* plays an important role in AgRP neurons by providing the metabolic flexibility to respond to metabolic information, particularly during fasting and the transition to refeeding, when the need to detect and respond to energy availability is most important. Our results show that *Crat* in AgRP neurons influences feeding behavior, hepatic substrates for gluconeogenesis and fatty acid metabolism, peripheral substrate utilization and nutrient partitioning, and the AgRP proteome during fasting and the transition to refeeding.

RESULTS

Validation of *Crat* Deletion in AgRP Neurons

We used a cre-lox approach to delete *Crat* from AgRP neurons. *Crat*-floxed mice (Muoio et al., 2012) were crossed to AgRP-ires-cre::NPY GFP mice to generate AgRP *Crat* wild-type (WT) and knockout (KO) mice that expressed GFP in neuropeptide Y (NPY) neurons. To confirm cre recombination in the arcuate (ARC) nucleus, WT and KO mice were crossed to *rosa26* tdTomato reporter mice (Figures 1A–1E) and we observed more than 90% of NPY GFP neurons expressing the AgRP cre-dependent tdTomato reporter (Figure 1D). We used a fluorescence-activated cell sorting (FACS) approach to isolate GFP-positive NPY neurons in the ARC coupled with nested PCR to confirm the deletion of *Crat* in NPY (AgRP) GFP-positive neurons. NPY GFP neurons from WT ($n = 5$) mice showed expected RNA transcripts for *Crat* at ~500 bp, whereas no *Crat* mRNA transcripts were observed in KO mice ($n = 5$) (Figure 1F). A stereological analysis showed no genotype differences in total NPY GFP neuronal number and cell volume at post-natal day 14 (P14), confirming that there were no adverse developmental effects on NPY cell number and volume in the ARC (Figures 1G–1I). No differences were observed in AgRP fiber density in the paraventricular nucleus (PVN), dorsomedial hypothalamic nucleus (DMH), or lateral hypothalamus (LH) between WT and KO mice (Figures 1J–1L). Likewise, we observed no differences in adrenal weight, adrenal histology, plasma corticosterone, and adrenal *Tyrosine hydroxylase* and *Agrp* mRNA content between genotypes (Figures S1A–S1H), an important observation because AgRP is also expressed in adrenal glands (Gupta et al., 2017).

Ad Libitum and Fasting-Induced Feeding Behavior

Under conditions of *ad libitum* access to food, there was no difference in average 24-hr food intake (Figures 2A and 2B). Intriguingly, despite no difference in total 24-hr food intake, the microstructure of feeding behavior was altered in KO mice with significantly shorter meal duration compared with WT mice but increased meal number to compensate (Figures 2C–2E). Because AgRP neurons promote food-seeking behavior during states of negative energy balance, we examined refeeding in

response to an overnight fast. KO mice exhibited significantly reduced cumulative food intake over a 24-hr period compared with WT control mice (Figures 2G and 2H), indicating an impaired feeding response after an overnight fast. Analysis of the microstructure of feeding behavior indicated that the first meal after refeeding was significantly smaller and that both average meal duration and meal size were significantly smaller compared with WT mice (Figures 2J and 2K). Collectively, these results show that deletion of *Crat* in AgRP neurons impairs refeeding after fasting and affects the microstructure of feeding behavior. There was no difference in body weight change or gastric emptying (Figures S2A and S2B) in WT and KO mice during fasting and refeeding.

Interestingly, there was no difference in the percentage of activated NPY neurons in WT or KO mice under fasted or refeed conditions (Figure 2N) using *fos* as a surrogate marker for activation in NPY GFP-labeled neurons. However, an increase in *fos*-positive neurons in non-NPY ARC neurons during refeeding (Figure 2O) suggests a greater sensitivity to potential satiety factors associated with refeeding. Body weight gain or fat mass over a 20-week chow diet or high-fat diet (HFD) feeding period did not differ between genotypes (Figures S3A to S3B). Analysis of metabolic parameters revealed no genotype differences in heat production, oxygen consumption (VO_2), or carbon dioxide production (VCO_2) on a chow diet (Figures S3C–S3E). High-fat diet-fed KO mice had an increase in heat production during both the light and dark phase relative to WT controls (Figure S3F), but this was not sufficient to influence adiposity. There were no genotype differences in VO_2 or VCO_2 (Figures S3G and S3H). There were also no differences in body weight change or total food intake after 5 days of leptin injections (Figures S3K and S3L).

Feeding Behavior in Response to Intraperitoneal CCK and ICV Insulin

Given that deletion of *Crat* in AgRP neurons decreased meal duration under *ad libitum* conditions, the possibility arises that KO mice were more sensitive to satiety signals. An injection of cholecystokinin (CCK) (0.25 μ g/kg, intraperitoneally [i.p.]) immediately before the dark phase (Figure 3A) highlighted that KO mice were more sensitive to i.p. CCK. KO mice exhibited reduced meal size and meal duration relative to WT mice (Figures 3B and 3C), but the meal number was significantly increased to compensate (Figure 3D). Hence, there was no overall difference in total food intake over the 24-hr period after CCK injection (Figure 3E).

Central insulin suppresses food intake (Brüning et al., 2000; Niswender et al., 2003), so we also injected insulin (0.025 μ U, intracerebroventricular [ICV]) into WT and KO mice and examined food intake and feeding behavior over a 24-hr period (Figure 3F). ICV insulin suppressed food intake in KO mice 2 hr after injection, an effect that was no longer evident by 6 hr or thereafter (Figures 3G and 3H). Analysis of 24-hr feeding behavior revealed that ICV insulin reduced meal size and meal duration and increased meal number in KO mice to compensate (Figures 3I–3K), resulting in no difference in 24-hr food intake between genotypes. These results are in accord with those of others (Campos et al., 2016), which highlight the ability of mice to adjust meal number to

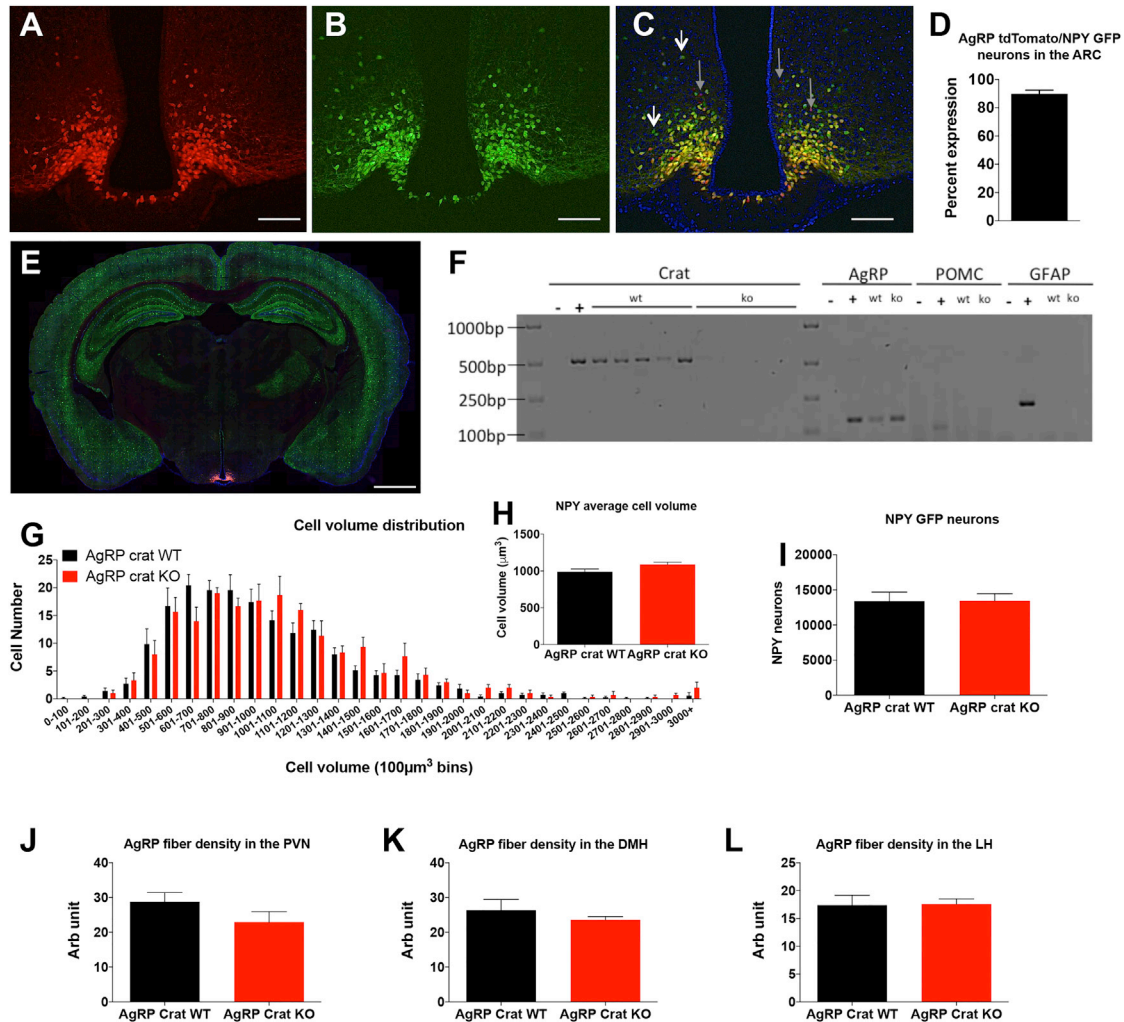


Figure 1. Validation of Cre-Mediated Recombination and Crat Deletion in AgRP Neurons

(A–D) Crossing AgRP-ires-cre::NPY GFP with rosa26-td-Tomato mice reveals that more than 90% of NPY neurons in the ARC express tdTomato as a marker of cre-dependent recombination in AgRP-expressing neurons. Scale bars, 200 μ m.

(E) Cre-dependent tdTomato expression only in the ARC; tiled montage; scale bar, 1 mm.

(F) FACS isolation of NPY-GFP neurons coupled with PCR analysis confirms no Crat mRNA transcripts in KO mice. *AgRP* mRNA transcript were observed, whereas neither proopiomelanocortin (*Pomc*) mRNA nor glial fibrillary acidic protein (*Gfap*) mRNA was observed from WT and KO mice.

(G–I) Stereological quantification of NPY GFP neurons confirms that neither cell number nor cell volume distribution was affected by Crat deletion during development.

(J–L) No differences in AgRP fiber density in the PVN (J), LH (K), and DMH (L).

All data are expressed as mean \pm SEM; n = 6–8.

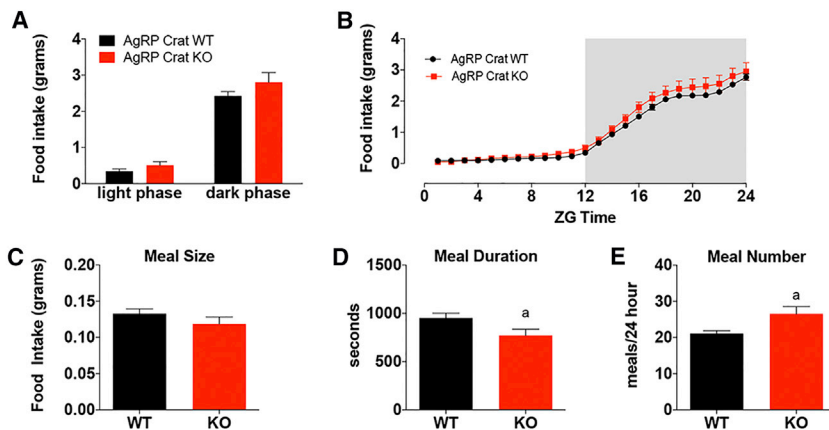
ensure constant 24-hr food intake (under *ad libitum* conditions) despite reduced meal size and duration.

In line with the feeding response to insulin, NPY (AgRP) neurons from KO mice showed greater sensitivity to exogenous insulin (i.p. 0.75 U/kg body weight), with a significant increase in insulin-induced phosphorylated AKT (pAKT) staining in NPY (AgRP) neurons compared with saline (Figure 3L). To further examine the physiological sensitivity of NPY (AgRP) neurons to insulin, we measured pAKT in NPY neurons 30 min after refeeding and observed significantly more NPY neurons expressing pAKT in KO mice compared with WT controls (Figure 3M).

AgRP Crat Deletion Causes a Metabolic Adaptation in Liver Function

Analysis of plasma in fed and fasted states revealed significantly lower concentrations of insulin and triglyceride (TG) in fasted KO mice compared with WT mice (Figures 3O and 3P). Fasting significantly increased plasma corticosterone, non-esterified fatty acids (NEFA), and ketone bodies in KO mice, but we found no significant genotype effect on blood glucose (Figures 3Q–3T). Although blood glucose was not different during fasting, the increased circulating ketone bodies indicated increased fatty acid oxidation and altered hepatic liver function in KO mice

Feeding behaviour: Ad libitum



Feeding behaviour: Fast/refeeding

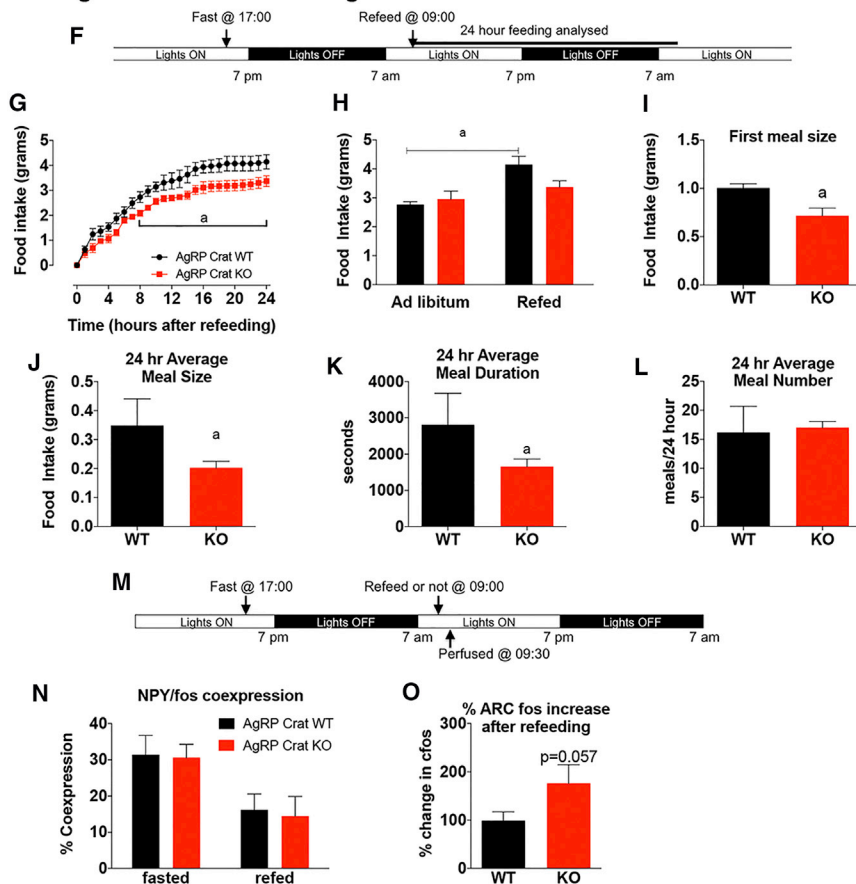


Figure 2. Deletion of Crat in AgRP Neurons Affects Feeding Behavior and Food Intake in Response to Fasting

(A–E) Deletion of Crat in AgRP neurons does not affect total food intake (A), cumulative food intake over a 24-hr period (B) and meal size (C); however, meal duration is reduced (D), and an increase in meal number (E) accounts for reduced meal duration.

(F–H) In response to fasting-refeeding (F), KO mice eat less than WT mice (G), and KO mice do not increase food intake relative to *ad libitum*-fed mice (H). (I–L) KO mice had a smaller first (I) and average meal size (J) and reduced meal duration (K) and no difference in meal number (L).

(M–O) Analysis of fos expression (M) demonstrated AgRP/NPY neurons from KO mice had a similar fos response to fasting refeeding (N), whereas overall fos activity in response to refeeding in the ARC was significantly increased in KO compared with WT (O).

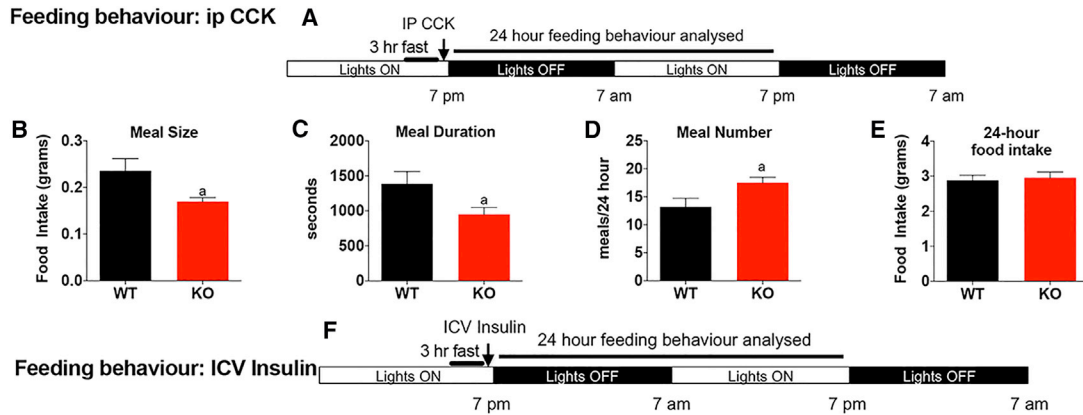
All data are expressed as mean \pm SEM; $n = 5$ –8. Two-way (repeated measures where appropriate) ANOVA with Tukey's *post hoc* analysis; a, significant at $p < 0.05$.

The accumulation of TG in the liver was unlikely to be due to increased *de novo* lipid synthesis because fatty acid synthase (*Fasn*) and stearoyl CoA desaturase (*Scd1*) were significantly suppressed in the fed state with no differences in the fasted state. Adipose TG lipase (*Atgl*), a marker of lipolysis, and carnitine palmitoyltransferase 1a (*Cpt1a*), a rate-limiting enzyme for acyl-CoA delivery into the mitochondrial matrix for oxidation, were elevated in fasted KO mice relative to fasted WT mice (Figure 4D). Liver fatty acid oxidation was also increased in KO mice (Figures 4E and 4F), which would account for the increased ketone bodies in the blood (Figure 3Q). Using a norepinephrine (NE) turnover approach (Joly-Amado et al., 2012), we showed little to no norepinephrine turnover in fasted KO mice and impaired norepinephrine turnover in the refeed state (Figures 4G and 4H), suggesting that inappropriate AgRP function in KO mice alters liver function by diminished sympathetic activity.

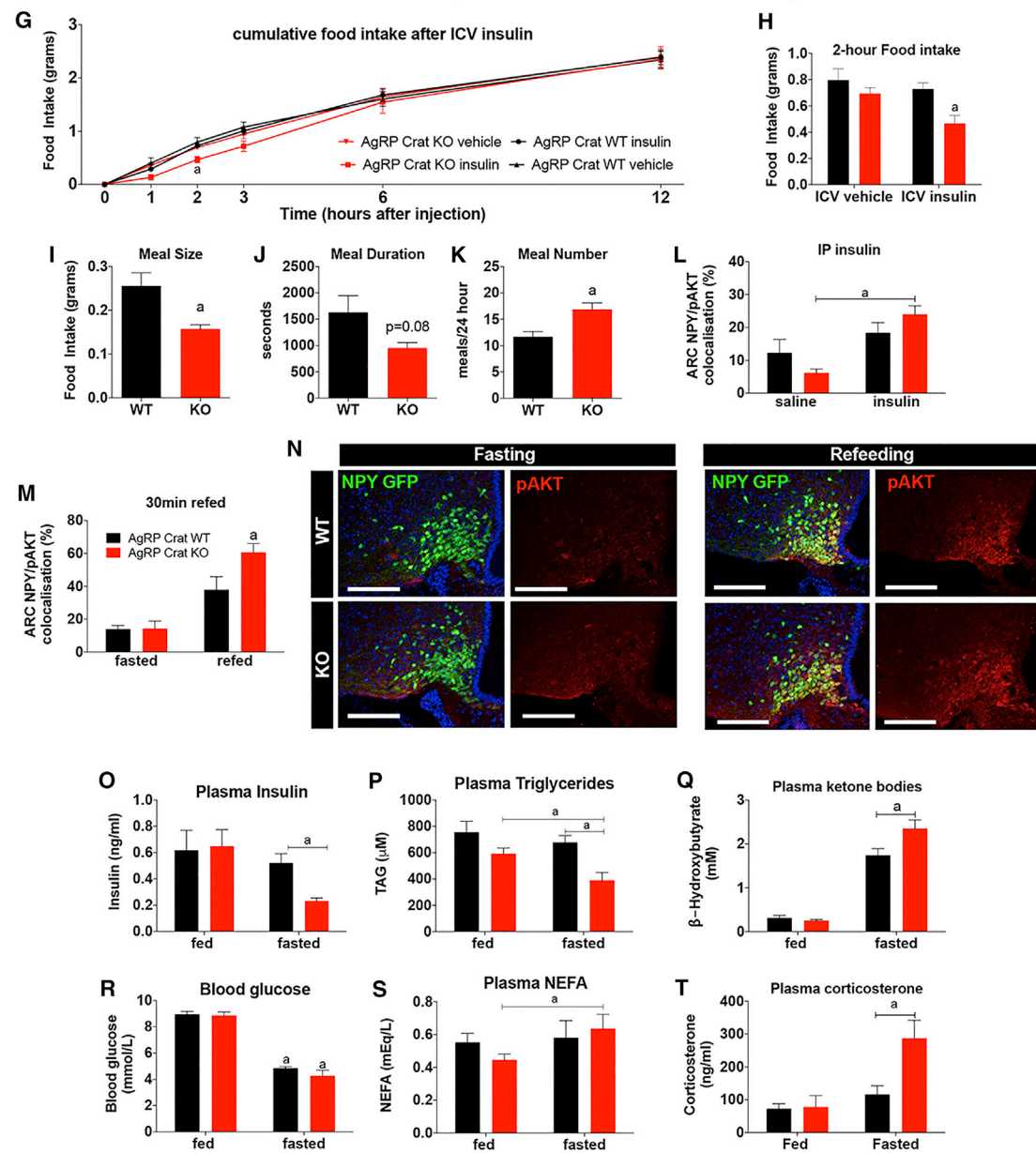
during fasting. In the fasted state, KO mice had significantly lower liver glycogen and higher TG concentrations relative to WT mice (Figure 4A–4C). The hepatic gluconeogenic genes *Pck1*, *Pck2*, and *G6pc* were significantly increased in fasted KO mice relative to fasted WT mice (Figure 4D), and, consistent with increased breakdown of liver glycogen, liver glycogen phosphorylase (*Pygl*) gene expression was significantly increased (Figure 4D).

The differences in liver glycogen and gluconeogenic genes in fasted KO mice suggest alterations in glycogenolysis and gluconeogenesis. In support of this, *Glycerol kinase* mRNA, the enzyme required to facilitate gluconeogenesis from glycerol, was significantly elevated in fasted KO mice (Figure 4D). Moreover, we investigated the fractional contribution of glycogenolysis and gluconeogenesis during fasting by employing a tracer-based approach to measure the sources of endogenous

Feeding behaviour: ip CCK



Feeding behaviour: ICV Insulin



(legend on next page)

glucose production (EGP). KO mice showed increased glycerol-driven gluconeogenesis after 3 hr fasting with a corresponding decrease in gluconeogenesis from phosphoenolpyruvate (Figures 4K and 4L). Moreover, blood glucose was significantly higher in KO mice compared with WT mice 15 min after an i.p. glycerol injection, indicating greater glycerol utilization for glucose production (Figure 4M). Collectively, our results suggest that the deletion of Crat from AgRP neurons affects the output of the sympathetic nervous system, which shifts liver metabolism to preferentially utilize glycerol as a substrate for gluconeogenesis.

AgRP Crat Deletion Acutely Impairs Glucose Tolerance

Initial experiments highlighted a greater increase in plasma glucose in KO compared with WT mice 15 and 30 min after oral glucose gavage (Figure 5A). Notably, blood glucose was not different between genotypes after 60 min, suggesting that AgRP Crat deletion may affect acute glycemic control rather than long-term regulation. Next we performed oral glucose tolerance tests (oGTTs) with stable isotope-labeled glucose (deuterated [6,6D₂] glucose), allowing the distinction between exogenous labeled glucose and unlabeled endogenous glucose in the blood. Our results showed significantly higher levels of labeled (exogenous) glucose in the plasma of KO mice, indicating reduced glucose disposal during the oral GTT (Figures 5C and 5D). Although there was no difference in the glucose concentration from endogenous sources over the course of 120 min, the rate of change from 0–15 minutes was significantly reduced in KO mice relative to WT mice (Figures 5E and 5F), indicating a diminished ability to suppress endogenous glucose production in that time. In addition, plasma insulin levels 5 and 10 min after glucose gavage were reduced compared with WT mice (Figure 5G), underpinning the reduced glucose disposal and reduced ability to suppress endogenous glucose production observed in KO mice.

We then performed a glucose uptake assay in various tissues to determine the capacity of the endogenous response to oral glucose to regulate glucose uptake. 15 min after glucose load, glucose uptake was lower in white adipose tissue (WAT) and skeletal muscle, with a paradoxical increase in the hypothalamus (Figure 5H). By 30 min after glucose load, all tissues showed greater glucose uptake in KO compared with WT mice (Figure 5I). Fos coexpression within ARC NPY GFP neurons was examined 10 min after an oral glucose load, which should reduce Fos coexpression in NPY neurons because their activity is reduced. The results showed more Fos-expressing NPY (AgRP) neurons in KO compared to WT mice (Figures 5J–5L), consistent with lack of suppression of Fos activity in response to a glucose

load. Collectively, these results suggest that the deletion of Crat from AgRP neurons attenuates their ability to acutely sense glucose and engage the appropriate mechanisms to clear plasma glucose within a 30-min time frame.

AgRP Crat Deletion Impairs Peripheral Nutrient Partitioning

KO mice showed a shift toward increased fatty acid utilization with a lower respiratory exchange ratio (RER) during both light and dark phases of the day (Figures 6A and 6B) when fed an *ad libitum* chow diet. In addition, heatmap analysis of RER values from individual mice clearly shows reduced RER values during fasting and refeeding (Figures 6C and 6D). Importantly, the change in RER in response to refeeding was delayed in KO mice, suggesting that the deletion of Crat from AgRP neurons influences peripheral nutrient partitioning to incoming nutrient availability. In line with greater fatty acid utilization, KO mice showed a greater clearance of lipids from the plasma following an olive oil gavage (Figure 6G). Moreover, we observed an adipose tissue (inguinal white fat) gene expression profile that would predict increased lipolysis in a fasted state (Figure 6H), which is consistent with increased plasma NEFA levels during fasting in KO mice (Figure 3S). Specifically, we observed an increase in KO mice in *Atgl* and lipoprotein lipase (*Lpl*), which hydrolyze TGs in intracellular lipid droplets and lipoproteins, respectively. Similarly, protein kinase A (*Pka*), an enzyme induced by adrenergic stimulation that increases lipolysis and phosphoglycolate phosphatase (*Pgp*), an enzyme required to liberate glycerol by dephosphorylating glycerol-3-phosphate (Mugabo et al., 2016), were both increased in KO mice. We also performed a lipoprotein lipase inhibition assay using tyloxapol (300 mg/kg body weight i.p. after a 5-hr fast) (Schotz et al., 1957) and observed a significant increase in plasma TG in KO mice (Figure 6I), suggesting greater efflux from the liver for utilization in peripheral tissues such as muscle. Indeed, the increased muscle TG concentration in the fed state shown in Figure 6J and increased plasma TG concentration in KO mice 3 hr after refeeding (Figure S2E) support this idea as a mechanism to restock muscle lipid content. We also observed that fasting increased *Pgp* mRNA expression, muscle glycogen phosphorylase (*Pygm*), and *Glut4*, whereas there was no increase in *Cpt1b* (Figure 6K). Norepinephrine turnover was reduced in fasted KO mice but significantly increased in refeed KO mice compared with WT controls (Figures 6L and 6M) underlying altered communication between the central nervous system and muscle in KO mice. Collectively, these studies show that Crat is required in AgRP neurons to regulate nutrient partitioning by regulating fatty acid utilization, gene expression, and metabolism.

Figure 3. Sensitivity to Insulin and CCK

(A–K) CCK (0.25 μg/kg, i.p.) (A) or insulin (0.025 μU, ICV) (F) produced smaller meal size (B and I), shorter meal duration (C and J) with a compensatory increase in meal number (D and K) in KO mice compared with WT controls. As a result, there were no differences in overall food intake 24 hr after CCK injections (E) and no differences 6 hr after insulin injections (G), although KO mice had significantly lower food intake 2 hr after ICV insulin administration (H).

(L–N) Analysis of pAKT staining in AgRP/NPY neurons 10 min after exogenous insulin injection (0.75 U/kg, i.p.) (L) or 30 min after refeeding (M) showed that KO mice have a higher sensitivity to circulating insulin. Representative micrographs of NPY/pAKT coexpression ARC sections during fasting and 30 min after refeeding (the white bar represents 100 μm) (N).

(O–T) Analysis of plasma insulin (O), triglycerides (P), ketone bodies (Q), glucose (R), NEFA (S), and corticosterone (T) from fed and fasted AgRP Crat mice.

All data are expressed as mean ± SEM; n = 7; a, significant at p < 0.05.

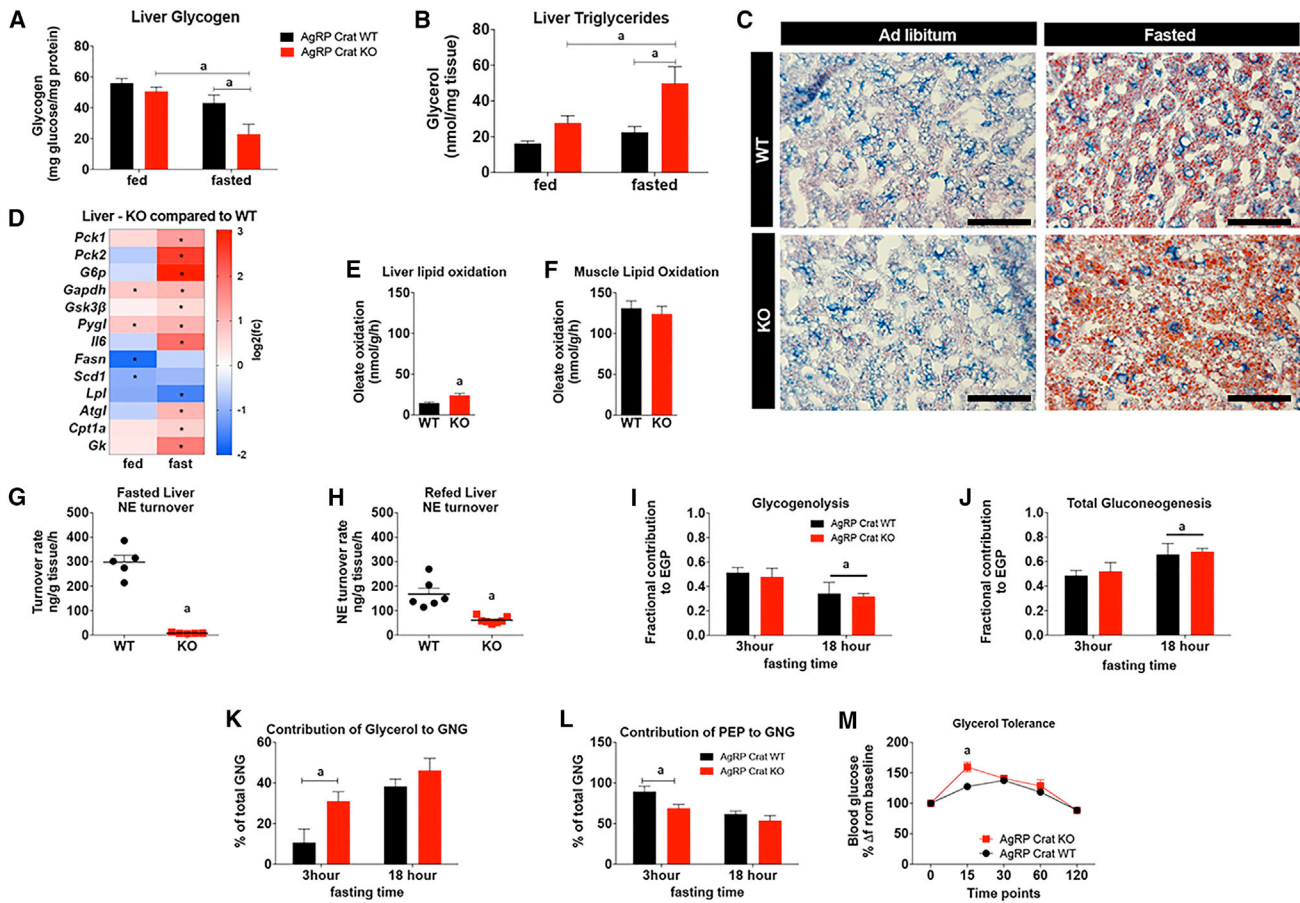


Figure 4. Deletion of Crat in AgRP Neurons Affects Peripheral Metabolism

(A) Liver glycogen was significantly reduced in KO mice relative to WT mice during fasting. (B and C) Liver triglycerides (B) were significantly increased in fasted KO mice compared with WT mice (C); Scale bars, 100 μ m. (D) KO liver mRNA levels as log₂ fold expression relative to WT controls. (E and F) *Ex vivo* analysis of fasted liver (E) and soleus muscle (F) oleate oxidation. (G and H) Noradrenaline turnover in fasted (G) and refed (H) liver. (I–L) Analysis of the fractional contribution of glycogenolysis (I) and gluconeogenesis (J) to endogenous glucose production, as well as the contribution of glycerol (K) and PEP (L) to gluconeogenesis, during fasting using heavy water coupled with mass spectrometry. (M) Blood glucose measurements after i.p. glycerol injection to assess glycerol tolerance.

atgl, adipose triglyceride lipase; Cpt1a, carnitine palmitoyltransferase 1a; Fasn, fatty acid synthase; G6p, glucose-6-phosphatase, catalytic; Gapdh, glyceraldehyde-3-phosphate dehydrogenase; Gk, glycerol kinase, transcript variant 1; Gsk3 β , glycogen synthase kinase 3 beta; IL-6, interleukin 6; Lpl, lipoprotein lipase; Pck1, phosphoenolpyruvate carboxykinase 1 (cytosol); Pck2, phosphoenolpyruvate carboxykinase 2 (mitochondrial); Pygl, glycogen phosphorylase, liver; Scd1, stearoyl-coenzyme A desaturase 1. All data are expressed as mean \pm SEM; n = 7–10. Two-way (repeated measures where appropriate) ANOVA with Tukey's post hoc analysis; a, significant at p < 0.05.

Crat Deletion Changes the AgRP Proteomic Response to Fasting and Refeeding

To examine how Crat deletion in AgRP neurons affects intracellular protein expression during fasting and refeeding, we used a FACS approach to collect NPY GFP neurons from WT and KO mice under fed, fasted, and refed conditions and analyzed protein abundance using mass spectrometry (Figure 7A). A comparison of WT versus KO mice under fed conditions revealed 32 proteins with a significant difference in abundance. Of these 32, 7 were more than 2-fold higher in NPY neurons, and 3 were more than 2-fold lower in NPY neurons from KO versus WT mice (Figure 7B; Table S1). Of the 32 proteins, 10 were grouped

into metabolic pathways (KEGG pathways ID 1100) (Figure 7C), and 3 were grouped to glycolysis (KEGG pathway ID 10). Two proteins within the metabolic KEGG pathway that were more than 2-fold higher in KO were NADH dehydrogenase 1 alpha subcomplex subunit 2 (Ndufa2) and methylenetetrahydrofolate dehydrogenase (Mthfd1), an oxidoreductase that can use nicotinamide adenine dinucleotide (NAD+) or nicotinamide adenine dinucleotide phosphate (NADP+) as acceptors.

In the fasted state, we identified 131 significantly different proteins in KO compared with WT NPY neurons. Of these 131, 84 were more than 2-fold higher, and 17 were more than 2-fold decreased (Table S2). KEGG identified 79 enriched pathways

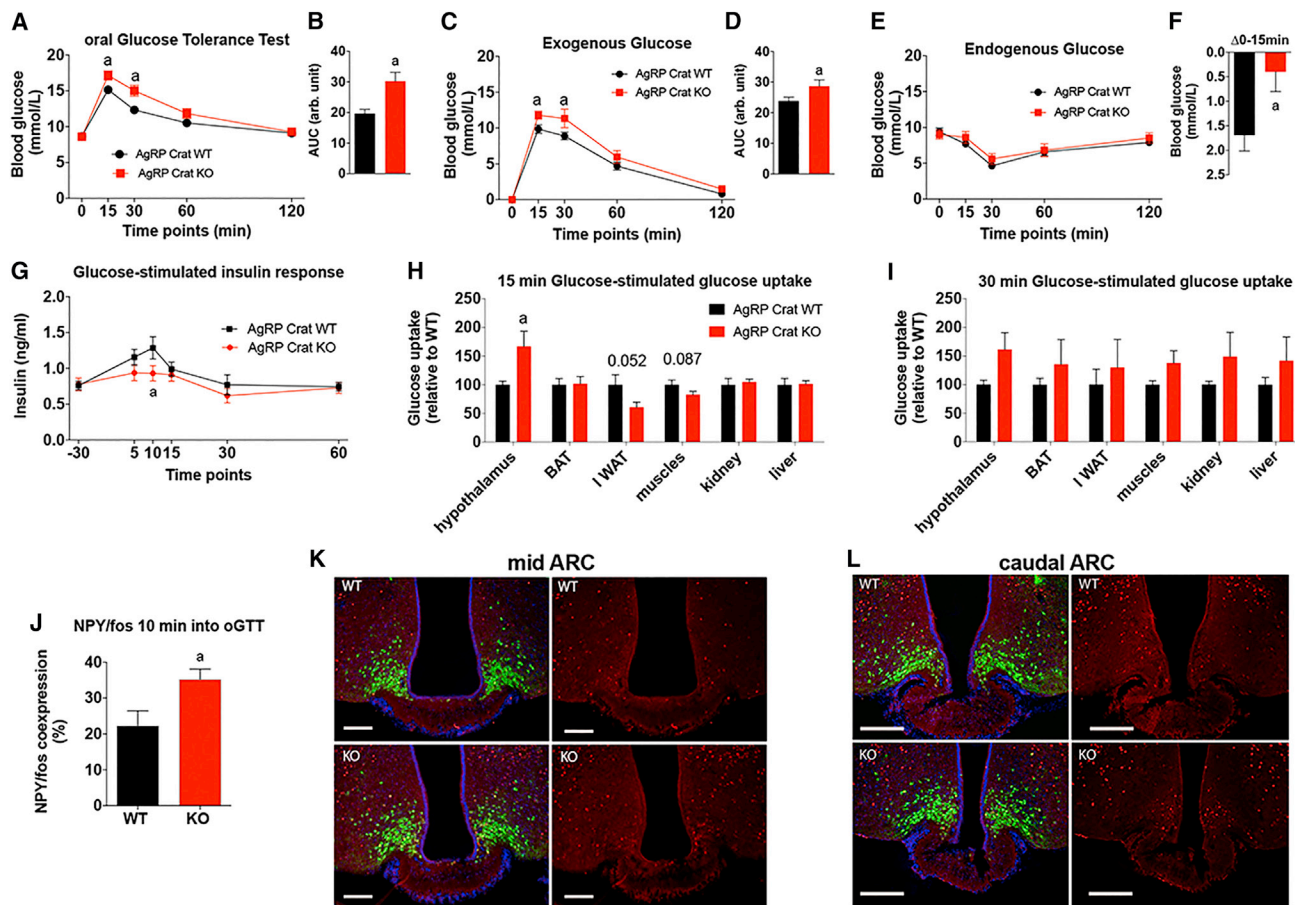


Figure 5. Deletion of Crat in AgRP Neurons Affects Glucose Homeostasis

(A and B) Oral GTT (1.5 g/kg) after 5 hr of fasting (A) and area under the curve (AUC) analysis (B). (C–E) Labeled oral GTT allows an estimate of exogenous glucose from gavage (C), with AUC (D) versus endogenous glucose from hepatic gluconeogenesis (E). (F) The change in blood glucose after 15 min after glucose gavage. (G) Glucose-stimulated insulin release during the oral GTT. (H and I) Glucose-stimulated glucose uptake after 15 min (H) and 30 min (I). (J) Analysis of fos-positive AgRP/NPY neurons 10 min after glucose gavage. (K and L) Representative micrographs of mid ARC (K) and caudal ARC (L) sections. Left: an overlay of the green channel (NPY-GFP) with the red (cos) from the right. Top: WT. Bottom: KO. Scale bars, 100 μ m. All data are expressed as mean \pm SEM; n = 7–10. Two-way (repeated measures where appropriate) ANOVA with Tukey's *post hoc* analysis; a, significant at $p < 0.05$.

with metabolic pathways (32 of 131) the most enriched (Figure 7D). The two most significantly increased proteins in KO versus WT NPY neurons in the fasted state were mitochondrial cytochrome b-c1 complex subunit 6 (Uqcrrh) and ATP-dependent 6-phosphofructokinase, platelet type (Pfkfb3), which catalyzes the third step of glycolysis. The 2 most significantly decreased proteins in NPY neurons from KO versus WT mice were NADH dehydrogenase (ubiquinone) Fe-S protein 6 (Ndufs6) and ATP synthase, H⁺ transporting, mitochondrial F1F0 complex, subunit e (Atp5k1). For a complete list, see Table S2.

During refeeding, we observed 190 significantly different proteins in KO versus WT NPY neurons. Of these 190, 39 were more than 2-fold increased, and 47 were more than 2-fold decreased in NPY neurons from KO versus WT mice. KEGG identified 59 enriched pathways, many of which were similar to those reported

in the fasted group, including the enrichment of the metabolic pathway (50 of 190) (Figure 7E; Table S3). The 2 most significantly increased metabolic pathway proteins in NPY neurons from KO versus WT mice were NADH dehydrogenase (ubiquinone) 1 subunit C2 (Ndufc2) and dolichyl-diphosphooligosaccharide protein (Rpn1). The 3 most significantly decreased proteins in NPY neurons from KO versus WT mice were ATP synthase protein 8 (Mtatp8), arginase 1 (Arg-1), and NADH dehydrogenase (ubiquinone) Fe-S protein 6 (Ndufs6).

Because acetyl CoA is the sole donor of acetyl groups for acetylation (Pietrocola et al., 2015), Crat may play an important indirect role in intracellular acetylation of proteins. Therefore, we examined whether Crat deletion affected the protein acetylation signature within NPY neurons from KO versus WT mice. Our results indicated that, under fed conditions, 14.15% versus

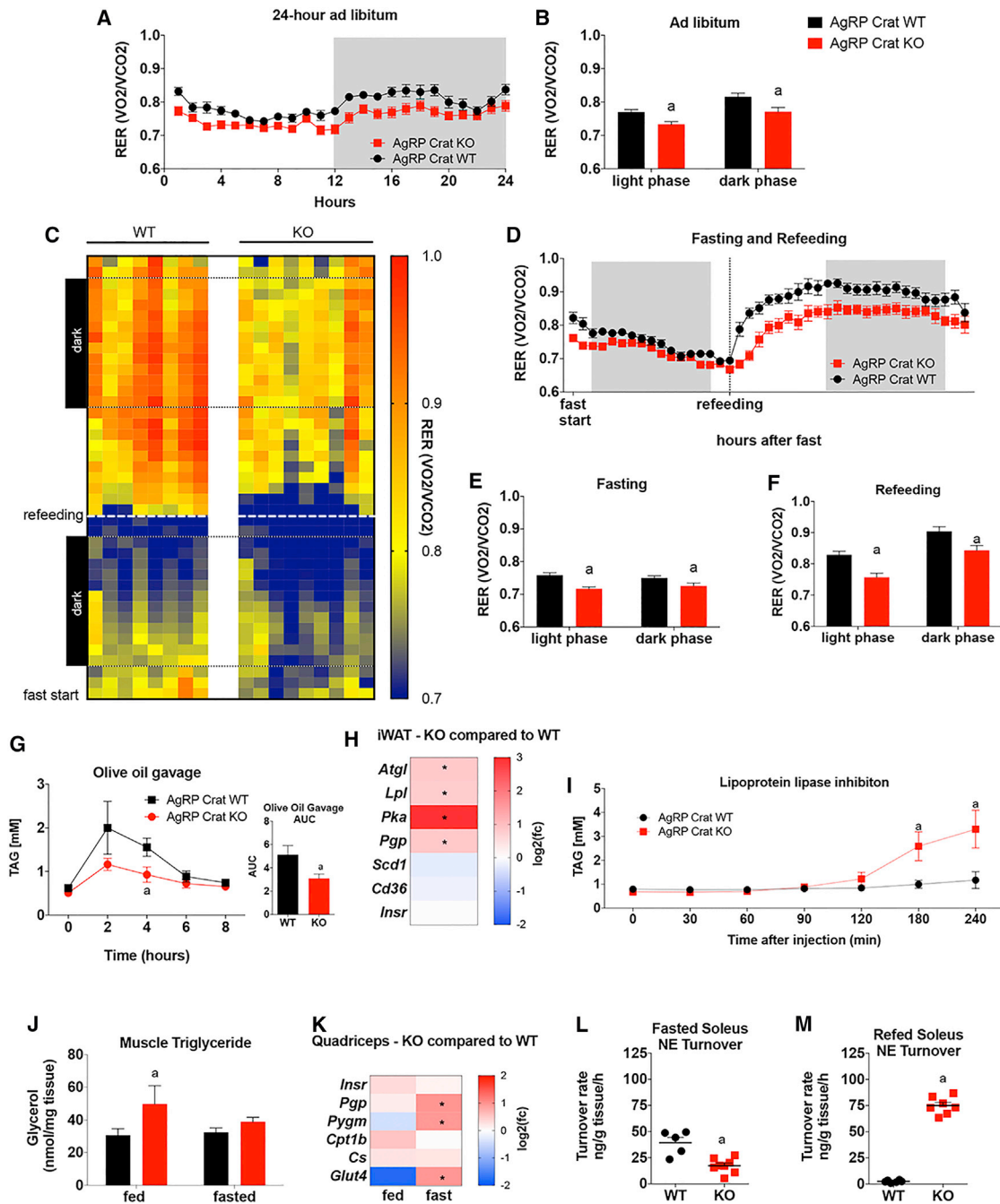


Figure 6. AgRP Crat Deletion Impairs Peripheral Nutrient Partitioning

(A–F) KO mice have a lower respiratory quotient (RER) under *ad libitum* conditions (A and B) and during fasting and refeeding (C–F). Each column of the heatmap represents one animal, and each row represents the average RER per hour; black boxes on the left side represent the dark phase, with black dotted lines indicating the change in light conditions. The white line represents the time point of refeeding. KO mice have a delayed switch from fatty acid to glucose utilization.

(G) KO mice showed greater TG clearance after olive oil load.

(H) KO iWAT mRNA levels as log₂ fold expression relative to WT controls.

(I) KO mice exhibit greater plasma TG levels after inhibiting LPL with tyloxapol (300 mg/kg body weight).

(J) Muscle triglycerides are significantly increased in fed KO mice compared with WT mice.

(K) KO muscle mRNA levels as log₂ fold expression relative to WT controls.

(L and M) Noradrenaline turnover in fasted and refed muscle.

CD36, CD36 antigen, transcript variant 1; *Cpt1b*, carnitine palmitoyltransferase 1b; *Cs*, citrate synthase; *Glut4*, glucose transporter 4; *InsR*, insulin receptor; *Pgp*, phosphoglycolate phosphatase; *Pka*, protein kinase A; *Pygm*, glycogen phosphorylase, muscle. All data are expressed as mean ± SEM; n = 7–10. Two-way (repeated measures where appropriate) ANOVA with Tukey's *post hoc* analysis; a, significant at p < 0.05.

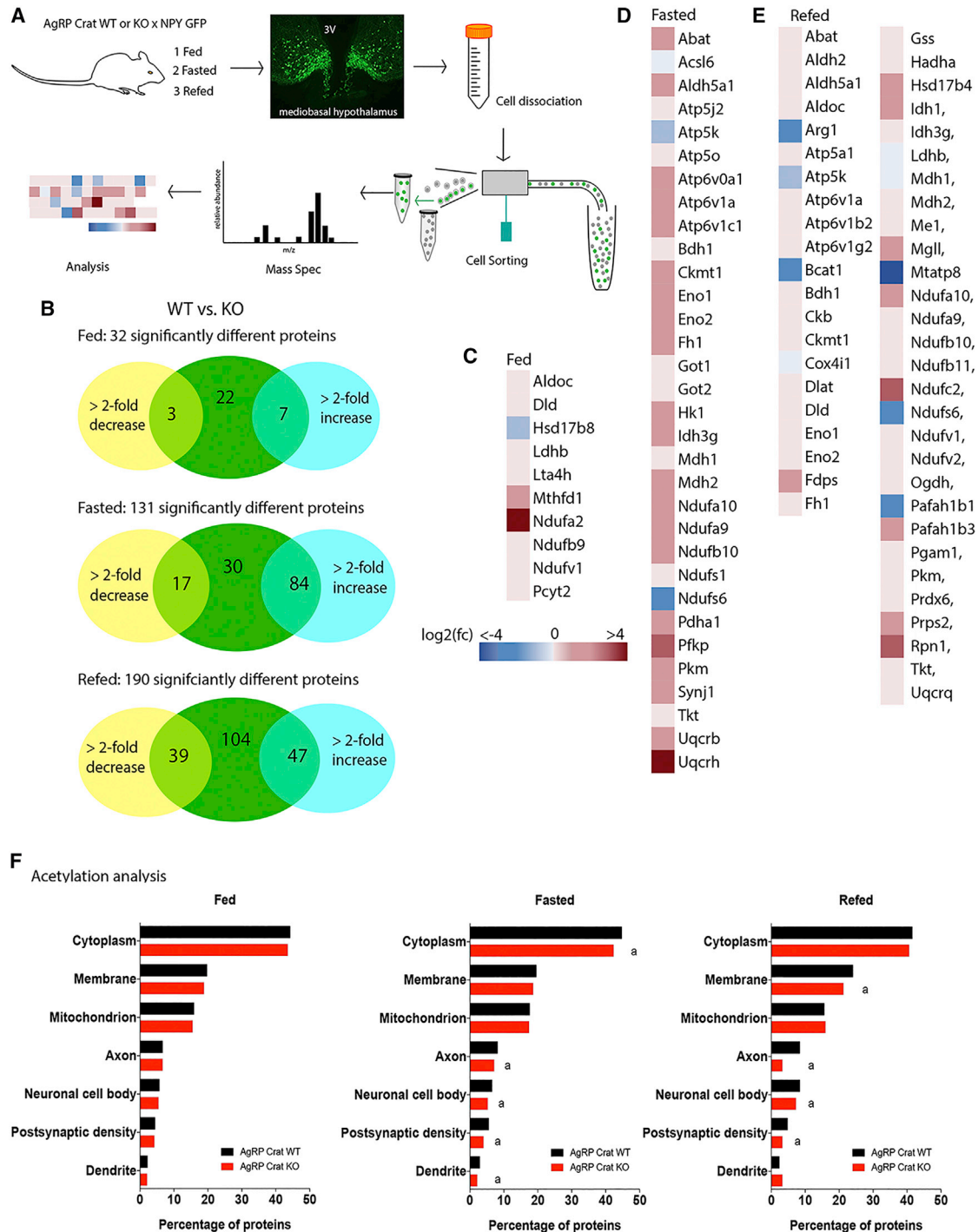


Figure 7. Crat Deletion Affects Protein Regulation in AgRP Neurons

(A) Hypothalami of mice under fed, fasted, and refed conditions were dissociated, and NPY GFP-positive cells were sorted by FACS for proteomic analysis.

(B) Significantly changed proteins were subjected to enrichment analysis using string database 10.0.

(C–E) The KEGG metabolic pathway had the highest enrichment under fed (C), fasted (D), and refed conditions (E).

(F) Enrichment analysis of acetylated proteins using FunRich 3.0 revealed that fewer proteins in KO are acetylated in the fasted and refed state.

Abat, 4-aminobutyrate aminotransferase; Acsl6, acyl-CoA synthetase long-chain family member 6; Aldh2, aldehyde dehydrogenase 2, mitochondrial; Aldh5a1, aldehyde dehydrogenase family 5, subfamily A1; Aldoc, aldolase C, fructose-bisphosphate; Arg1, arginase, liver; Atp5a1, ATP synthase, H⁺ transporting, mitochondrial F1 complex, alpha subunit 1; Atp5j2, ATP synthase, H⁺ transporting, mitochondrial F0 complex, subunit F2; Atp5k, ATP synthase, H⁺ transporting, mitochondrial F1F0 complex, subunit e; Atp5o, ATP synthase, H⁺ transporting, mitochondrial F1 complex, O subunit; Atp6v0a1, ATPase,

(legend continued on next page)

13.80% of proteins were acetylated in WT and KO NPY neurons, respectively (Figure 7F). However, under conditions of fasting, 15.03% of proteins in WT NPY neurons were acetylated, whereas this was significantly lower at 13.88% in KO NPY neurons ($p < 0.05$). Under refed conditions, 15.06% and 13.61% of proteins were acetylated from WT and KO NPY neurons ($p < 0.05$), respectively (Figure 7F).

DISCUSSION

AgRP activation engages neural circuits to prevent and/or adapt to states of hunger by promoting energy conservation and euglycemia. However, the ability of AgRP neurons to acutely respond to signals of incoming energy availability is also important to conserve energy, as illustrated by increased fatty acid utilization and attenuated body weight gain on a HFD in AgRP neonatally ablated mice (Joly-Amado et al., 2012). This nutrient partitioning involves effectively and rapidly switching off peripheral fatty acid oxidation in favor of storage, characteristic of the transition from a fasted to a refed state. Our current studies suggest that Crat affects AgRP neuronal function predominantly during fasting and the transition to refeeding. This is based on observations in which the deletion of Crat in AgRP neurons changes food intake and feeding behavior after fasting; hepatic function during fasting, which includes a shift to glycerol as a preferred gluconeogenic substrate; peripheral glucose clearance in response to an acute glucose load; peripheral fatty acid oxidation during fasting and in response to refeeding; and the intracellular protein abundance and acetylation status within AgRP neurons, particularly during fasting and refeeding. Thus, the influence of Crat on AgRP neuronal function is most relevant during fasting and in the transition to refeeding. This occurs at a time when metabolic processing in AgRP neurons is most relevant to control nutrient partitioning to promote maximal energy conservation.

Although a large amount of literature has focused on the important role of AgRP neurons to increase energy-conserving mechanisms during fasting, little research has focused on the mechanisms that enable AgRP neurons to respond to acute

refeeding. In muscle, Crat regulates metabolic flexibility by facilitating the substrate switch during the transition from fasting to refeeding (Muio et al., 2012; Seiler et al., 2015). These actions attenuate the development of metabolic diseases such as obesity and type 2 diabetes. Our results show that Crat in AgRP neurons is required to maintain metabolic flexibility during the transition from fasting to refeeding and suggest a distinct function of Crat in substrate switching, irrespective of tissue type. KO mice not only showed increased fatty acid utilization during *ad libitum* and fasted conditions, as indicated by the lower RER, they also showed a blunted switch from fatty acid to glucose utilization during the fasting-to-refeeding transition. Moreover, the deletion of Crat in AgRP neurons improves whole-body glycerol and TG handling and the response to lipoprotein lipase inhibition in the same manner as AgRP ablation (Joly-Amado et al., 2012). Although this did not influence body fat loss during a single bout of fasting, we predict that this would affect energy homeostasis during a model of chronic energy deficit, such as calorie restriction or feeding entrainment, when AgRP neurons are most important to restore energy homeostasis (Andermann and Lowell, 2017).

The importance of Crat in AgRP neurons to maintain metabolic flexibility and nutrient partitioning was also observed after glucose administration because blood glucose was significantly higher in KO mice 15 and 30 min after gavage, primarily because of impaired glucose clearance, but returned to levels in WT mice at 60 and 120 min. Together with RER changes, these results show that Crat blunts, but does not prevent, the responsiveness of AgRP neurons. This observation is supported by measures of glucose-stimulated glucose uptake, which shows deficits in glucose uptake in inguinal white adipose tissue (iWAT) and muscle at 15 min but not at 30 min. Interestingly, it is after this 30-min time point that glucose clearance is no longer different in WT and KO mice during an oral GTT.

Crat deletion affected the acetylation profile of proteins within AgRP neurons during fasting and refeeding but not in the fed state, which further highlights the important role of Crat in AgRP neurons during fasting-to-refeeding transition. This is

H⁺ transporting, lysosomal V0 subunit A1; Atp6v1a, ATPase, H⁺ transporting, lysosomal V1 subunit A; Atp6v1b2, ATPase, H⁺ transporting, lysosomal V1 subunit B2; Atp6v1c1, ATPase, H⁺ transporting, lysosomal V1 subunit C1; Atp6v1g2, ATPase, H⁺ transporting, lysosomal V1 subunit G2; Bcat1, branched chain aminotransferase 1, cytosolic; Bdh1, 3-hydroxybutyrate dehydrogenase, type 1; Ckb, creatine kinase, brain; Ckmt1, creatine kinase, mitochondrial 1, ubiquitous; Cox4i1, cytochrome c oxidase subunit IV isoform 1; Dlat, dihydrolipoamide S-acetyltransferase (E2 component of pyruvate dehydrogenase complex); Dld, dihydrolipoamide dehydrogenase; Eno1, enolase 1, alpha non-neuron; Eno2, enolase 2, gamma neuronal; Fdps, farnesyl diphosphate synthetase; Fh1, fumarate hydratase 1; Got1, glutamate oxaloacetate transaminase 1, soluble; Got2, glutamate oxaloacetate transaminase 2, mitochondrial; Gss, glutathione synthetase; H2-Ke6, H2-K region expressed gene 6; Hadha, hydroxyacyl-coenzyme A dehydrogenase/3-ketoacyl-coenzyme A thiolase/enoyl-coenzyme A hydratase (trifunctional protein), alpha subunit; Hk1, hexokinase 1; Hsd17b4, hydroxysteroid (17-beta) dehydrogenase 4; Idh1, isocitrate dehydrogenase 1 (NADP+), soluble; Idh3g, isocitrate dehydrogenase 3 (NAD+), gamma; Ldhb, lactate dehydrogenase B; Lta4h, leukotriene A4 hydrolase; Mdh1, malate dehydrogenase 1, NAD (soluble); Mdh2, malate dehydrogenase 2, NAD (mitochondrial); Me1, malic enzyme 1, NADP(+)-dependent, cytosolic; Mgl1, monoglyceride lipase; mt-Atp8, mitochondrially encoded ATP synthase 8; Mthfd1, methylenetetrahydrofolate dehydrogenase (NADP+ dependent), methenyltetrahydrofolate cyclohydrolase, formyltetrahydrofolate synthase; Ndufa10, NADH dehydrogenase (ubiquinone) 1 alpha subcomplex 10; Ndufa2, NADH dehydrogenase (ubiquinone) 1 alpha subcomplex, 2; Ndufa9, NADH dehydrogenase (ubiquinone) 1 alpha subcomplex, 9; Ndufb10, NADH dehydrogenase (ubiquinone) 1 beta subcomplex, 10; Ndufb11, NADH dehydrogenase (ubiquinone) 1 beta subcomplex, 11; Ndufb9, NADH dehydrogenase (ubiquinone) 1 beta subcomplex, 9; Ndufc2, NADH dehydrogenase (ubiquinone) 1, subcomplex unknown, 2; Ndufs1, NADH dehydrogenase (ubiquinone) Fe-S protein 1; Ndufs6, NADH dehydrogenase (ubiquinone) Fe-S protein 6; Ndufv1, NADH dehydrogenase (ubiquinone) flavoprotein 1; Ndufv2, NADH dehydrogenase (ubiquinone) flavoprotein 2; Ogdh, oxoglutarate dehydrogenase (lipoamide); Pafah1b1, platelet-activating factor acetylhydrolase, isoform 1b, subunit 1; Pafah1b3, platelet-activating factor acetylhydrolase, isoform 1b, subunit 3; Pcyt2, phosphate cytidyltransferase 2, ethanolamine; Pdh1, pyruvate dehydrogenase E1 alpha 1; Pfkfb, phosphofructokinase, platelet; Pgam1, phosphoglycerate mutase 1; Pkm, pyruvate kinase, muscle; Prdx6, peroxiredoxin 6; Prps2, phosphoribosyl pyrophosphate synthetase 2; Rpn1, ribophorin I; Synj1, synaptotagmin 1; Tkt, transketolase; Uqcrb, ubiquinol-cytochrome c reductase binding protein; Uqcrl, ubiquinol-cytochrome c reductase hinge protein; Uqcrc, ubiquinol-cytochrome c reductase, complex III subunit VII.

consistent with others who showed that Crat plays an important role in intracellular acetylation of proteins (Davies et al., 2016; Madiraju et al., 2009) by regulating acetyl group availability for acetylation (Pietrocola et al., 2015). Further analysis of proteomic data highlighted that Crat regulates metabolic processing primarily during fasting and refeeding. Differentially regulated proteins included those involved in sirtuin (SIRT) activity, NADH metabolism, uncoupling activity, glycolysis, and mitochondrial dynamics. We also noted a number of differences related to proteins involved in synaptic function and endocytosis. This supports the concept that increased synaptic activity requires greater energetic demands via mitochondrial transport (Li et al., 2004), dynamics (Dietrich et al., 2013), and appropriate mitochondrial processing. Although a number of proteins regulating mitochondrial function are known to influence AgRP function and energy homeostasis, including mitofusins (Dietrich et al., 2013), AMP-activated protein kinase (AMPK) (Claret et al., 2007), SIRT (Dietrich et al., 2010), PGC1 α (Gill et al., 2016), and uncoupling protein-2 (Andrews et al., 2008), none of these studies have illustrated the importance of AgRP metabolic pathways during fasting and the refeeding transition.

Because AgRP neurons play a fundamental role in food intake, we examined the effects of Crat deletion on food intake and feeding behavior. Under *ad libitum* conditions, meal duration was significantly reduced; however, animals increased the meal number so that overall food intake was not different between genotypes. These results are consistent with Campos et al. (2016), in which inactivation of a subpopulation of AgRP to parabrachial calcitonin gene-related peptide (CGRP) neurons (AgRP \rightarrow CGRP^{PBeI}) reduced meal duration but mice were able to increase the meal number to maintain appropriate food intake. Moreover, this study showed that the inability to engage the AgRP \rightarrow CGRP^{PBeI} pathway heightened sensitivity to satiety cues (Campos et al., 2016), consistent with our observations that KO mice are more sensitive to feedback signals of satiety (i.p. CCK and ICV insulin). AgRP neurons projecting to the lateral hypothalamus, anterior bed nucleus of the *stria terminalis*, PVN, and paraventricular thalamus also increase the drive to eat (Betley et al., 2013) independent from the AgRP \rightarrow CGRP^{PBeI} pathway, and elevated AgRP neuronal activity during fasting is required to elicit positive valence after MC4R^{PVN} activation (Garfield et al., 2015). Thus, under conditions of hunger, as seen in fasted mice, AgRP neurons promote energy intake by simultaneously increasing food intake and suppressing the actions of satiety signals. Indeed, Crat deletion occurs in 90% of ARC NPY neurons, suggesting impaired pathways driving food intake and the AgRP \rightarrow CGRP^{PBeI} pathway that suppresses meal termination. Consistent with this, fasted KO mice exhibit reduced food intake during refeeding and smaller meal size and duration.

Although there was no difference in fasting blood glucose between genotypes, our results indicate that, during fasting, the deletion of Crat from AgRP neurons forces the liver to generate glucose using glycerol as a substrate for gluconeogenesis. Hepatic glycogen depletion during fasting in humans increases glycerol as a substrate for gluconeogenesis, an effect dependent on an increase in lipolysis (Jahoor et al., 1992). Indeed, we observed greater glycogen depletion in fasted KO mice, supporting the concept that KO mice shift more quickly to glycerol

as a gluconeogenic substrate and show greater fatty acid oxidation. This change occurs without affecting the rates of glycogenolysis and total gluconeogenesis and suggests that a simple endpoint measurement of blood glucose is not sufficient to address the biological adaptive mechanisms that ensure euglycemia. Importantly, gluconeogenesis from glycerol requires a constant rate of glycerol supply (Samuel and Shulman, 2016), and we observed significantly greater TG concentrations in the liver and plasma NEFA in fasted KO mice, a phenomenon also witnessed in AgRP-ablated mice (Joly-Amado et al., 2012). Our data indicate that greater hepatic fatty acid oxidation (gene expression, functional enzyme activity, and ketone bodies) in fasted KO mice reflects the need to break down TG to supply glycerol for gluconeogenesis. We also observed an increase in phosphoglycerate phosphatase (*pgp*) mRNA in adipose tissue, the enzyme required for glycerol release from adipocytes (Mugabo et al., 2016).

In summary, our studies show that AgRP neurons require Crat to regulate metabolic flexibility and peripheral nutrient partitioning during fasting and the transition to refeeding, similar to a known role of Crat in skeletal muscle (Muoio et al., 2012; Seiler et al., 2015). The metabolic flexibility required to acutely switch from fatty acid to glucose utilization during refeeding represents an important mechanism that helps store energy-rich fatty acids and maximizes energy conservation until required. We suggest that Crat in AgRP neurons is required for metabolic processing, as shown by a number of intracellular proteomic changes, to allow AgRP neurons to respond to changing metabolic states, particularly during “active” fasting states and during the transition to refeeding, which requires “acute inhibition” of AgRP neurons (Wu et al., 2014). Moreover, Crat within AgRP neurons engages sympathetic outflow in response to changing metabolic states, which, in turn, coordinates peripheral organs to optimize nutrient partitioning. The inability to properly adapt to changing metabolic substrates is clearly an important mechanism affecting the development of obesity-related diseases, including diabetes and dyslipidemia. Beyond calorie intake, it is becoming clear that the inappropriate handling of nutrient “fate” is largely responsible for metabolic disease, and this study shows that Crat in AgRP neurons has an unappreciated role in this process.

EXPERIMENTAL PROCEDURES

Animals

All experiments were conducted in compliance with the Monash University Animal Ethics Committee guidelines. Male mice were kept under standard laboratory conditions with free access to food (chow diet, catalog no. 8720610, Barastoc Stockfeeds, Victoria, Australia) and water at 23°C in a 12-hr light/dark cycle and were group-housed to prevent isolation stress unless otherwise stated. All male mice were aged 8 weeks or older for experiments unless otherwise stated. Additional information about animals can be found in the Supplemental Experimental Procedures.

Food Intake Experiments

Mice were single-housed in specialized feeding cages (BioDAQ, Research Diets, NJ, USA), and recordings were analyzed after a 3-day acclimation period. Feeding behavior after fasting and short-term fasting (3 hr) combined with i.p. CCK (0.25 μ g/kg) or ICV insulin (0.025 μ U in 1.5 μ L) administered at the onset of the active period were analyzed.

Metabolic Studies

For labeled or unlabeled oral GTTs (1.5 g/kg) and glycerol tolerance test (GlyTT, 1 g/kg i.p.), mice were fasted from 8 a.m., and tests were performed 5 hr later, at 1 p.m. Labeled glucose enrichment in plasma samples was measured via gas chromatography-mass spectrometry (GC-MS) (for details, see the [Supplemental Experimental Procedures](#)).

Endogenous Glucose Production

Mice were injected with deuterated water (D₂O) (0.9% NaCl in D₂O, 25 mL/kg bodyweight, i.p.) and 10% D₂O mixed into drinking water. Five hours after injection, mice were subjected to a fast, and plasma samples (20 μ L) were taken after 3 and 18 hr of fasting. Enrichment was measured via GC-MS (Kowalski et al., 2015; [Supplemental Experimental Procedures](#)).

Glucose-Stimulated Glucose Uptake

To localize glucose uptake in tissue, we performed oral GTT (1.5g/kg) combined with intraperitoneal injection of tritiated 2-deoxy-D-glucose (2-(3H)-DG) tracer (10 μ Ci in 200 μ L saline; see the [Supplemental Experimental Procedures](#) for details).

CLAMS

To assess the energy expenditure of AgRP Crat mice during *ad libitum* chow feeding, fasting, and refeeding and HFD conditions, single-housed mice were placed in a comprehensive lab animal monitoring system (Oxymax-CLAMS), and recordings were analyzed after a 1-day acclimation period.

Analysis of Blood Chemistry

Detailed protocols can be found in the [Supplemental Experimental Procedures](#).

PCR

Total RNA was extracted from tissue with Qiazol (Qiazol Sciences) according to the instruction manual (see the [Supplemental Experimental Procedures](#) for a detailed description of the procedure). cDNA synthesis and real-time qPCR were performed as described previously (Stark et al., 2015b). For primer details, see the [Supplemental Experimental Procedures](#).

Ex Vivo Fat Oxidation Assay

Animals were anesthetized with isoflurane. Tissues were collected and incubated in Krebs buffer containing 14C-oleate (1 μ Ci/mL), and 14CO₂ was captured in 1 M NaOH for a period of 2 hr and measured as described previously (Meex et al., 2015).

Norepinephrine Turnover

Norepinephrine was measured by high performance liquid chromatography (HPLC), and turnover rates were calculated after log transformation by $\log(\text{saline}) - \log(\text{alpha-methyl-p-tyrosine [aMPT]}) / 0.434$, where 0.434 is an estimate for the kinetic rate (Brodie et al., 1966; for details; see the [Supplemental Experimental Procedures](#)).

Proteomics of AgRP Neurons

Peptides were analyzed using nano liquid chromatography-mass spectrometry (for details, see the [Supplemental Experimental Procedures](#)). Acquired .raw files were analyzed with MaxQuant (v1.5.5.1) to globally identify and quantify proteins across the different conditions. Data visualization and statistical analyses were performed in Perseus (v1.5.5.3). After removing the reversed and known contaminating proteins, the label-free quantification (LFQ) values were log₂-transformed, and the reproducibility across the biological replicates was evaluated by Pearson's correlation analysis. The replicates were grouped into WT fed versus KO fed, WT fasted versus KO fasted, and WT refed versus KO refed. A two-sample t test was performed to obtain the significantly expressed proteins, with $p < 0.05$. Significantly changed proteins were further analyzed to investigate association with KEGG pathways and gene ontology (GO) terms using the String database. Enrichment analysis for compartmentalization of acetylated proteins was performed against the Uniprot database (rodents, taxon ID 9989) with FunRich 3.0.

Immunohistochemistry

Immunohistochemistry was performed as reported previously (Wu et al., 2014) using the following primary antibodies: c-Fos rabbit polyclonal immunoglobulin G (IgG) (sc-52, Santa Cruz Biotechnology) and phospho-AKT (Ser473) rabbit monoclonal IgG (9271s, Cell Signaling Technology). The secondary antibody for both was Alexa Fluor goat anti-rabbit 594 antibody (A-11037, Invitrogen). Fiber density, cell number, and volume were measured with a design-based unbiased stereology method (StereoInvestigator, MicroBrightField, VT, USA) as described previously (Lemus et al., 2015).

Statistical Analysis

Statistical analyses were performed using GraphPad Prism for MacOS X. Data are represented as mean \pm SEM. Two-way ANOVAs with *post hoc* tests were used to determine statistical significance. A two-tailed Student's unpaired t test was used when comparing genotype only. $p < 0.05$ was considered statistically significant.

SUPPLEMENTAL INFORMATION

Supplemental Information includes Supplemental Experimental Procedures, three figures, and three tables and can be found with this article online at <https://doi.org/10.1016/j.celrep.2018.01.067>.

ACKNOWLEDGMENTS

We thank Minh Deo technical assistance. We acknowledge Monash FlowCore for sorting of cells using FACS. We acknowledge use of the facilities at the Monash Biomedical Proteomics Facility and the Monash Histology Platform. We thank Doug Compton from Research Diets for helping to set up and establish BioDAQ feeding cages. This study was supported by an Australian NHMRC grant and fellowship (1126724 and 1084344 to Z.B.A. and APP1077703 to M.J.W.). This work used the PBRC Transgenic Core, which is supported in part by COBRE (NIH 8P20GM103528) and NORC (NIH 2P30-DK072476-11A1) center grants from the NIH. A.R. is supported by an Australian Government Research Training Program scholarship. J.F.G. is the recipient of funding from Conselho Nacional de Desenvolvimento Científico e Tecnológico-CNPq Brazil.

AUTHOR CONTRIBUTIONS

A.R. and Z.B.A. conceived the idea, designed and performed the experiments, analyzed data, and wrote the manuscript. Z.B.A. supervised and coordinated the project. G.M.K., C.R.B., R.B.S., B.J.O., S.L., and M.J.W. helped design experiments. R.S., R.E.C., S.H.L., C.H., M.B.L., J.F.G., G.M.K., C.R.B., M.M., S.L., R.R.G.D., and M.J.W. contributed to performing experiments. R.L.M. provided the Crat floxed mouse model. A.R., M.J.W., S.L., and Z.B.A. discussed the results and edited the manuscript. All authors read and approved the manuscript.

DECLARATION OF INTERESTS

The authors declare no competing interests.

Received: April 14, 2017

Revised: November 13, 2017

Accepted: January 22, 2018

Published: February 13, 2018

REFERENCES

- Andermann, M.L., and Lowell, B.B. (2017). Toward a wiring diagram understanding of appetite control. *Neuron* 95, 757–778.
- Andrews, Z.B. (2011). Central mechanisms involved in the orexigenic actions of ghrelin. *Peptides* 32, 2248–2255.
- Andrews, Z.B., Liu, Z.W., Wallingford, N., Erion, D.M., Borok, E., Friedman, J.M., Tschöp, M.H., Shanabrough, M., Ciine, G., Shulman, G.I., et al. (2008).

- UCP2 mediates ghrelin's action on NPY/AgRP neurons by lowering free radicals. *Nature* *454*, 846–851.
- Aponte, Y., Atasoy, D., and Sternson, S.M. (2011). AGRP neurons are sufficient to orchestrate feeding behavior rapidly and without training. *Nat. Neurosci.* *14*, 351–355.
- Baskin, D.G., Breininger, J.F., and Schwartz, M.W. (1999). Leptin receptor mRNA identifies a subpopulation of neuropeptide Y neurons activated by fasting in rat hypothalamus. *Diabetes* *48*, 828–833.
- Betley, J.N., Cao, Z.F., Ritola, K.D., and Sternson, S.M. (2013). Parallel, redundant circuit organization for homeostatic control of feeding behavior. *Cell* *155*, 1337–1350.
- Briggs, D.I., Lemus, M.B., Kua, E., and Andrews, Z.B. (2011). Diet-induced obesity attenuates fasting-induced hyperphagia. *J. Neuroendocrinol.* *23*, 620–626.
- Brodie, B.B., Costa, E., Diabac, A., Neff, N.H., and Smookler, H.H. (1966). Application of steady state kinetics to the estimation of synthesis rate and turnover time of tissue catecholamines. *J. Pharmacol. Exp. Ther.* *154*, 493–498.
- Brüning, J.C., Gautam, D., Burks, D.J., Gillette, J., Schubert, M., Orban, P.C., Klein, R., Krone, W., Müller-Wieland, D., and Kahn, C.R. (2000). Role of brain insulin receptor in control of body weight and reproduction. *Science* *289*, 2122–2125.
- Campos, C.A., Bowen, A.J., Schwartz, M.W., and Palmiter, R.D. (2016). Parabrachial CGRP neurons control meal termination. *Cell Metab.* *23*, 811–820.
- Claret, M., Smith, M.A., Batterham, R.L., Selman, C., Choudhury, A.I., Fryer, L.G., Clements, M., Al-Qassab, H., Heffron, H., Xu, A.W., et al. (2007). AMPK is essential for energy homeostasis regulation and glucose sensing by POMC and AgRP neurons. *J. Clin. Invest.* *117*, 2325–2336.
- Davies, M.N., Kjalarsdottir, L., Thompson, J.W., Dubois, L.G., Stevens, R.D., Ilkayeva, O.R., Brosnan, M.J., Rolph, T.P., Grimsrud, P.A., and Muoio, D.M. (2016). The acetyl group buffering action of carnitine acetyltransferase offsets macronutrient-induced lysine acetylation of mitochondrial proteins. *Cell Rep.* *14*, 243–254.
- Dietrich, M.O., Antunes, C., Geliang, G., Liu, Z.W., Borok, E., Nie, Y., Xu, A.W., Souza, D.O., Gao, Q., Diano, S., et al. (2010). Agrp neurons mediate Sirt1's action on the melanocortin system and energy balance: roles for Sirt1 in neuronal firing and synaptic plasticity. *J. Neurosci.* *30*, 11815–11825.
- Dietrich, M.O., Liu, Z.W., and Horvath, T.L. (2013). Mitochondrial dynamics controlled by mitofusins regulate Agrp neuronal activity and diet-induced obesity. *Cell* *155*, 188–199.
- Enriori, P.J., Evans, A.E., Sinnayah, P., Jobst, E.E., Tonelli-Lemos, L., Billes, S.K., Glavas, M.M., Grayson, B.E., Perello, M., Nillni, E.A., et al. (2007). Diet-induced obesity causes severe but reversible leptin resistance in arcuate melanocortin neurons. *Cell Metab.* *5*, 181–194.
- Garfield, A.S., Li, C., Madara, J.C., Shah, B.P., Webber, E., Steger, J.S., Campbell, J.N., Gavrilova, O., Lee, C.E., Olson, D.P., et al. (2015). A neural basis for melanocortin-4 receptor-regulated appetite. *Nat. Neurosci.* *18*, 863–871.
- Gill, J.F., Delezie, J., Santos, G., and Handschin, C. (2016). PGC-1 α expression in murine AgRP neurons regulates food intake and energy balance. *Mol. Metab.* *5*, 580–588.
- Gropp, E., Shanabrough, M., Borok, E., Xu, A.W., Janoschek, R., Buch, T., Plum, L., Balthasar, N., Hampel, B., Waisman, A., et al. (2005). Agouti-related peptide-expressing neurons are mandatory for feeding. *Nat. Neurosci.* *8*, 1289–1291.
- Gupta, R., Ma, Y., Wang, M., and Whim, M.D. (2017). AgRP-expressing edrenal chromaffin cells are involved in the sympathetic response to fasting. *Endocrinology* *158*, 2572–2584.
- Jahoor, F., Klein, S., and Wolfe, R. (1992). Mechanism of regulation of glucose production by lipolysis in humans. *Am. J. Physiol.* *262*, E353–E358.
- Joly-Amado, A., Denis, R.G., Castel, J., Lacombe, A., Cansell, C., Rouch, C., Kassis, N., Dairou, J., Cani, P.D., Ventura-Clapier, R., et al. (2012). Hypothalamic AgRP-neurons control peripheral substrate utilization and nutrient partitioning. *EMBO J.* *31*, 4276–4288.
- Kleinridders, A., Könnner, A.C., and Brüning, J.C. (2009). CNS-targets in control of energy and glucose homeostasis. *Curr. Opin. Pharmacol.* *9*, 794–804.
- Könnner, A.C., Janoschek, R., Plum, L., Jordan, S.D., Rother, E., Ma, X., Xu, C., Enriori, P., Hampel, B., Barsh, G.S., et al. (2007). Insulin action in AgRP-expressing neurons is required for suppression of hepatic glucose production. *Cell Metab.* *5*, 438–449.
- Kowalski, G.M., Kloehn, J., Burch, M.L., Selathurai, A., Hamley, S., Bayol, S.A., Lamon, S., Watt, M.J., Lee-Young, R.S., McConville, M.J., and Bruce, C.R. (2015). Overexpression of sphingosine kinase 1 in liver reduces triglyceride content in mice fed a low but not high-fat diet. *Biochim. Biophys. Acta* *1851*, 210–219.
- Krashes, M.J., Koda, S., Ye, C., Rogan, S.C., Adams, A.C., Cusher, D.S., Maratos-Flier, E., Roth, B.L., and Lowell, B.B. (2011). Rapid, reversible activation of AgRP neurons drives feeding behavior in mice. *J. Clin. Invest.* *121*, 1424–1428.
- Lemus, M.B., Bayliss, J.A., Lockie, S.H., Santos, V.V., Reichenbach, A., Stark, R., and Andrews, Z.B. (2015). A stereological analysis of NPY, POMC, Orexin, GFAP astrocyte, and Iba1 microglia cell number and volume in diet-induced obese male mice. *Endocrinology* *156*, 1701–1713.
- Li, Z., Okamoto, K., Hayashi, Y., and Sheng, M. (2004). The importance of dendritic mitochondria in the morphogenesis and plasticity of spines and synapses. *Cell* *119*, 873–887.
- Luquet, S., Perez, F.A., Hnasko, T.S., and Palmiter, R.D. (2005). NPY/AgRP neurons are essential for feeding in adult mice but can be ablated in neonates. *Science* *310*, 683–685.
- Madiraju, P., Pande, S.V., Prentki, M., and Madiraju, S.R. (2009). Mitochondrial acetylcarnitine provides acetyl groups for nuclear histone acetylation. *Epigenetics* *4*, 399–403.
- Meex, R.C., Hoy, A.J., Morris, A., Brown, R.D., Lo, J.C.Y., Burke, M., Goode, R.J.A., Kingwell, B.A., Kraakman, M.J., Febbraio, M.A., et al. (2015). Fetuin B is a secreted hepatocyte factor linking steatosis to impaired glucose metabolism. *Cell Metab.* *22*, 1078–1089.
- Mugabo, Y., Zhao, S., Seifried, A., Gezzar, S., Al-Mass, A., Zhang, D., Lamon-tagne, J., Attane, C., Poursharifi, P., Iglesias, J., et al. (2016). Identification of a mammalian glycerol-3-phosphate phosphatase: Role in metabolism and signaling in pancreatic β -cells and hepatocytes. *Proc. Natl. Acad. Sci. USA* *113*, E430–E439.
- Muoio, D.M., Noland, R.C., Kovalik, J.P., Seiler, S.E., Davies, M.N., DeBalsi, K.L., Ilkayeva, O.R., Stevens, R.D., Kheterpal, I., Zhang, J., et al. (2012). Muscle-specific deletion of carnitine acetyltransferase compromises glucose tolerance and metabolic flexibility. *Cell Metab.* *15*, 764–777.
- Niswender, K.D., Morrison, C.D., Clegg, D.J., Olson, R., Baskin, D.G., Myers, M.G., Jr., Seeley, R.J., and Schwartz, M.W. (2003). Insulin activation of phosphatidylinositol 3-kinase in the hypothalamic arcuate nucleus: a key mediator of insulin-induced anorexia. *Diabetes* *52*, 227–231.
- Pietrocola, F., Galluzzi, L., Bravo-San Pedro, J.M., Madeo, F., and Kroemer, G. (2015). Acetyl coenzyme A: A central metabolite and second messenger. *Cell Metab.* *21*, 805–821.
- Ramsay, R.R., and Zammit, V.A. (2004). Carnitine acyltransferases and their influence on CoA pools in health and disease. *Mol. Aspects Med.* *25*, 475–493.
- Ruan, H.B., Dietrich, M.O., Liu, Z.W., Zimmer, M.R., Li, M.D., Singh, J.P., Zhang, K., Yin, R., Wu, J., Horvath, T.L., and Yang, X. (2014). O-GlcNAc transferase enables AgRP neurons to suppress browning of white fat. *Cell* *159*, 306–317.
- Samuel, V.T., and Shulman, G.I. (2016). The pathogenesis of insulin resistance: integrating signaling pathways and substrate flux. *J. Clin. Invest.* *126*, 12–22.
- Schotz, M.C., Scanu, A., and Page, I.H. (1957). Effect of triton on lipoprotein lipase of rat plasma. *Am. J. Physiol.* *188*, 399–402.
- Schwartz, M.W., Erickson, J.C., Baskin, D.G., and Palmiter, R.D. (1998). Effect of fasting and leptin deficiency on hypothalamic neuropeptide Y gene transcription in vivo revealed by expression of a lacZ reporter gene. *Endocrinology* *139*, 2629–2635.
- Seiler, S.E., Koves, T.R., Gooding, J.R., Wong, K.E., Stevens, R.D., Ilkayeva, O.R., Wittmann, A.H., DeBalsi, K.L., Davies, M.N., Lindeboom, L., et al.

(2015). Carnitine acetyltransferase mitigates metabolic inertia and muscle fatigue during exercise. *Cell Metab.* *22*, 65–76.

Stark, R., Reichenbach, A., and Andrews, Z.B. (2015a). Hypothalamic carnitine metabolism integrates nutrient and hormonal feedback to regulate energy homeostasis. *Mol. Cell. Endocrinol.* *418*, 9–16.

Stark, R., Reichenbach, A., Lockie, S.H., Pracht, C., Wu, Q., Tups, A., and Andrews, Z.B. (2015b). Acyl ghrelin acts in the brain to control liver function and peripheral glucose homeostasis in male mice. *Endocrinology* *156*, 858–868.

van de Wall, E., Leshan, R., Xu, A.W., Balthasar, N., Coppari, R., Liu, S.M., Jo, Y.H., MacKenzie, R.G., Allison, D.B., Dun, N.J., et al. (2008). Collective and in-

dividual functions of leptin receptor modulated neurons controlling metabolism and ingestion. *Endocrinology* *149*, 1773–1785.

Wang, Q., Liu, C., Uchida, A., Chuang, J.C., Walker, A., Liu, T., Osborne-Lawrence, S., Mason, B.L., Moshier, C., Berglund, E.D., et al. (2013). Arcuate AgRP neurons mediate orexigenic and gluco-regulatory actions of ghrelin. *Mol. Metab.* *3*, 64–72.

Wu, Q., Lemus, M.B., Stark, R., Bayliss, J.A., Reichenbach, A., Lockie, S.H., and Andrews, Z.B. (2014). The temporal pattern of cfos activation in hypothalamic, cortical, and brainstem nuclei in response to fasting and refeeding in male mice. *Endocrinology* *155*, 840–853.